

Strange baryon spectroscopy in the relativistic quark model

R. N. Faustov and V. O. Galkin

*Dorodnicyn Computing Center, Federal Research Center “Computer Science and Control”,
Russian Academy of Sciences, Vavilov Str. 40, 119333 Moscow, Russia*

Mass spectra of strange baryons are calculated in the framework of the relativistic quark model based on the quasipotential approach. Baryons are treated as the relativistic quark-diquark bound systems. It is assumed that two quarks with equal constituent masses form a diquark. The diquark excitations and its internal structure are consistently taken into account. Calculations are performed up to rather high orbital and radial excitations of strange baryons. On this basis the Regge trajectories are constructed. The obtained results are compared with available experimental data and previous predictions. It is found that all masses of the 4- and 3-star, as well as most of the 2- and 1-star states of strange baryons with established quantum numbers are well reproduced. The developed relativistic quark-diquark model predicts less excited states than three-quark models of strange baryons.

PACS numbers: 14.20.Jn, 12.39.Ki, 12.39.Pn

I. INTRODUCTION

At present the extensive evidence (including lattice calculations) of the existence of diquark correlations in hadrons was collected.¹ It continues constantly growing with the accumulation of new data on various properties of light and heavy hadrons [1]. Thus recently several charged charmonium- and bottomonium-like states were discovered [1, 2]. They should be inevitably multi-quark, at least four quark — tetraquark, states. One of the most successful pictures of such tetraquark states is the diquark-antidiquark model [3, 4]. In the light meson sector it has been argued for a long time that mesons forming the inverted lightest scalar nonet can be well described as tetraquarks [5] treated as diquark-antidiquark bound states [6, 7]. In the baryon sector it is well known that the number of observed excited states both in the light and heavy sectors is considerably lower than the number of excited states predicted in the three-quark picture [8–11]. The introduction of diquarks significantly reduces this number of baryon states since in such a picture some of degrees of freedom are frozen and thus the number of possible excitations is substantially smaller.

In our previous papers we developed the relativistic quark-diquark model of doubly heavy [12] and heavy baryons [13, 14]. We assumed that two heavy quarks in a doubly heavy baryon and two light quarks in a heavy baryon form a diquark. The relativistic quasipotential equation with the QCD-motivated quark-quark interaction was solved for obtaining diquark characteristics, such as the diquark masses and form factors. The calculation of the diquark form factors is necessary for taking into account the diquark internal structure. For doubly heavy diquarks [12] we considered both ground and excited states, while for light diquarks [13] we limited ourselves by only ground state scalar and axial vector diquarks. Then the

¹ A vast literature on this subject is available. Therefore we mostly refer to the recent reviews where the references to earlier review and original papers can be found.

baryon masses were calculated by solving the relativistic quark-diquark equation. It was found that the heavy baryon spectra are well described in the proposed approach [13, 14]. The calculated baryon wave functions were used for the description of weak decays of the doubly heavy and heavy baryons in Refs. [15, 16].

Here we extend our relativistic quark-diquark model for the calculation of the mass spectra of strange baryons. These baryons are considered as the bound systems of a quark and diquark, where we assume that a diquark is composed from quarks of the same constituent mass. Thus Λ and Σ baryons contain the strange s quark and the light qq ($q = u, d$) diquark, while Ξ and Ω baryons contain the light q or strange s quark and the strange ss diquark. Our analysis of the strange baryon spectroscopy shows that it is necessary to consider both ground and excited states of these diquarks. As the result the number of obtained baryon states is increased, however it is still significantly less than in the three-quark approaches. The differences become evident for the higher quark excitations in a baryon. Our goal is to calculate the strange baryon spectra up to rather high orbital and radial excitations. On this basis the Regge trajectories for these baryons can be constructed and their linearity can be tested. Moreover, the comparison of the Regge trajectory slopes for strange and charmed baryons as well as light mesons can be made.

The paper is organized as follows. In Sec. II we briefly describe our relativistic quark-diquark model of baryons. Expressions for the quasipotentials of the quark-quark interaction in a diquark and the quark-diquark interaction in a baryon are given which include both the spin-independent and spin-dependent relativistic contributions. Masses and form factor parameters of ground and excited states of diquarks are calculated. In Sec. III the mass spectra of strange baryons are considered. The obtained results are confronted with available experimental data and predictions of other approaches. We calculate the strange baryon masses up to rather high orbital and radial excitations in the quark-diquark bound system. This allows us to construct their Regge trajectories which are presented in Sec. IV. The corresponding slopes and intercepts are determined. Finally, we give our conclusions in Sec. V.

II. RELATIVISTIC QUARK-DIQUARK MODEL

For the calculations of the strange baryon spectra we employ the quasipotential approach and quark-diquark picture of baryons which was previously used for the investigation of the heavy baryon spectroscopy [13, 14]. In our present analysis we closely follow these considerations. The interaction of two quarks in a diquark and the quark-diquark interaction in a baryon are described by the diquark wave function Ψ_d of the bound quark-quark state and by the baryon wave function Ψ_B of the bound quark-diquark state respectively, which satisfy the quasipotential equation of the Schrödinger type [17]

$$\left(\frac{b^2(M)}{2\mu_R} - \frac{\mathbf{p}^2}{2\mu_R} \right) \Psi_{d,B}(\mathbf{p}) = \int \frac{d^3q}{(2\pi)^3} V(\mathbf{p}, \mathbf{q}; M) \Psi_{d,B}(\mathbf{q}), \quad (1)$$

where the relativistic reduced mass is

$$\mu_R = \frac{M^4 - (m_1^2 - m_2^2)^2}{4M^3}, \quad (2)$$

and M is the bound state mass (diquark or baryon), $m_{1,2}$ are the masses of quarks (q_1 and q_2) which form the diquark or of the diquark (d) and quark (q) which form the baryon (B),

and \mathbf{p} is their relative momentum. In the center of mass system the relative momentum squared on mass shell reads

$$b^2(M) = \frac{[M^2 - (m_1 + m_2)^2][M^2 - (m_1 - m_2)^2]}{4M^2}. \quad (3)$$

The kernel $V(\mathbf{p}, \mathbf{q}; M)$ in Eq. (1) is the quasipotential operator of the quark-quark or quark-diquark interaction which is constructed with the help of the off-mass-shell scattering amplitude, projected onto the positive energy states. We assume that the effective interaction is the sum of the usual one-gluon exchange term and the mixture of long-range vector and scalar linear confining potentials, where the vector confining potential contains the Pauli term. The details can be found in Refs. [13, 14]. The resulting quasipotentials are given by the following expressions.

(a) Quark-quark (qq) interaction in the diquark

$$V(\mathbf{p}, \mathbf{q}; M) = \bar{u}_1(p)\bar{u}_2(-p)\mathcal{V}(\mathbf{p}, \mathbf{q}; M)u_1(q)u_2(-q), \quad (4)$$

with

$$\mathcal{V}(\mathbf{p}, \mathbf{q}; M) = \frac{1}{2} \left[\frac{4}{3} \alpha_s D_{\mu\nu}(\mathbf{k}) \gamma_1^\mu \gamma_2^\nu + V_{\text{conf}}^V(\mathbf{k}) \Gamma_1^\mu(\mathbf{k}) \Gamma_{2;\mu}(-\mathbf{k}) + V_{\text{conf}}^S(\mathbf{k}) \right],$$

(b) Quark-diquark (qd) interaction in the baryon

$$\begin{aligned} V(\mathbf{p}, \mathbf{q}; M) = & \frac{\langle d(P) | J_\mu | d(Q) \rangle}{2\sqrt{E_d(p)E_d(q)}} \bar{u}_q(p) \frac{4}{3} \alpha_s D_{\mu\nu}(\mathbf{k}) \gamma^\nu u_q(q) \\ & + \psi_d^*(P) \bar{u}_q(p) J_{d;\mu} \Gamma_q^\mu(\mathbf{k}) V_{\text{conf}}^V(\mathbf{k}) u_q(q) \psi_d(Q) \\ & + \psi_d^*(P) \bar{u}_q(p) V_{\text{conf}}^S(\mathbf{k}) u_q(q) \psi_d(Q), \end{aligned} \quad (5)$$

where α_s is the QCD coupling constant, $\langle d(P) | J_\mu | d(Q) \rangle$ is the vertex of the diquark-gluon interaction which takes into account the diquark internal structure and $J_{d;\mu}$ is the effective long-range vector vertex of the diquark. The diquark momenta are $P = (E_d(p), -\mathbf{p})$, $Q = (E_d(q), -\mathbf{q})$ with $E_d(p) = \sqrt{\mathbf{p}^2 + M_d^2}$. $D_{\mu\nu}$ is the gluon propagator in the Coulomb gauge, $\mathbf{k} = \mathbf{p} - \mathbf{q}$; γ_μ and $u(p)$ are the Dirac matrices and spinors, while $\psi_d(P)$ is the diquark wave function [13]. The factor 1/2 in the quark-quark interaction accounts for the difference of the colour factor compared to the quark-antiquark case.

The effective long-range vector vertex of the quark is defined by [17]

$$\Gamma_\mu(\mathbf{k}) = \gamma_\mu + \frac{i\kappa}{2m} \sigma_{\mu\nu} \tilde{k}^\nu, \quad \tilde{k} = (0, \mathbf{k}), \quad (6)$$

where κ is the anomalous chromomagnetic moment of quarks.

In the nonrelativistic limit the vector and scalar confining potentials reduce to

$$\begin{aligned} V_{\text{conf}}^V(r) &= (1 - \varepsilon)(Ar + B), \\ V_{\text{conf}}^S(r) &= \varepsilon(Ar + B), \end{aligned} \quad (7)$$

where ε is the mixing coefficient. Thus in this limit the usual Cornell-like potential is reproduced

$$V(r) = -\frac{4}{3} \frac{\alpha_s}{r} + Ar + B, \quad (8)$$

TABLE I: Masses M and form factor parameters of diquarks.

Quark content	I	State nl_j	M (MeV)	ξ (GeV)	ζ (GeV ²)
ud	0	$1s_0$	710	1.09	0.185
	1	$1s_1$	909	1.185	0.365
	0	$1p_0$	1321	1.395	0.148
	0	$1p_1$	1397	1.452	0.195
	0	$1p_2$	1475	1.595	0.173
	1	$1p_1$	1392	1.451	0.194
	0	$2s_0$	1513	1.01	0.055
	1	$2s_1$	1630	1.05	0.151
ss	0	$1s_1$	1203	1.13	0.280
	0	$1p_1$	1608	1.03	0.208
	0	$2s_1$	1817	0.805	0.235

where we use the QCD coupling constant with freezing

$$\alpha_s(\mu^2) = \frac{4\pi}{\beta_0 \ln \frac{\mu^2 + M_B^2}{\Lambda^2}}, \quad \beta_0 = 11 - \frac{2}{3}n_f, \quad \mu = \frac{2m_1m_2}{m_1 + m_2}, \quad (9)$$

with the background mass $M_B = 2.24\sqrt{A} = 0.95$ GeV [18] and $\Lambda = 413$ MeV [19].

All parameters of the model were fixed previously from calculations of meson and baryon properties [17]. The constituent quark masses $m_u = m_d = 0.33$ GeV, $m_s = 0.5$ GeV and the parameters of the linear potential $A = 0.18$ GeV² and $B = -0.3$ GeV have the usual values of quark models. The value of the mixing coefficient of vector and scalar confining potentials $\varepsilon = -1$ and the universal Pauli interaction constant $\kappa = -1$. Note that the long-range chromomagnetic contribution to the potential, which is proportional to $(1 + \kappa)$, vanishes for the chosen value of $\kappa = -1$.

First we calculate masses and form factors of the diquarks. The quasipotential equation (1) is solved numerically for the complete relativistic potential which depends on the diquark mass in a complicated highly nonlinear way [13]. In our approach we assume that diquarks in strange baryons are formed by the constituent quarks of the same mass, i.e. we consider only the ud , uu , dd and ss diquarks. Note that the ground state ud diquark can be both in scalar and axial vector state, while the ground state diquarks composed from quarks of the same flavour uu , dd and ss can be only in the axial vector state due to the Pauli principle. The obtained masses of the ground and excited states of diquarks are presented in Table I. The diquark state is characterized by the quark content, isospin I , radial quantum number $n = 1, 2, 3 \dots$, orbital momentum $l = s, p$ and total angular momentum $j = 0, 1, 2$ (the diquark spin). In this table we also give the values of the parameters ξ and ζ . They enter the vertex $\langle d(P) | J_\mu | d(Q) \rangle$ of the diquark-gluon interaction (5) which is parameterized by the form factor

$$F(r) = 1 - e^{-\xi r - \zeta r^2}, \quad (10)$$

that takes the internal diquark structure into account [13].

Next we calculate the masses of heavy baryons as the bound states of a quark and diquark. The quark-diquark potential is the sum of spin-independent and spin-dependent parts [13, 14]

$$V(r) = V_{\text{SI}}(r) + V_{\text{SD}}(r). \quad (11)$$

The spin-independent $V_{\text{SI}}(r)$ part is given by

$$\begin{aligned} V_{\text{SI}}(r) = & \hat{V}_{\text{Coul}}(r) + V_{\text{conf}}(r) + \frac{1}{E_d E_q} \left\{ \frac{1}{2} (E_q^2 - m_q^2 + E_d^2 - M_d^2) [\hat{V}_{\text{Coul}}(r) + V_{\text{conf}}^V(r)] \right. \\ & + \frac{1}{4} \Delta [2V_{\text{Coul}}(r) + V_{\text{conf}}^V(r)] + \hat{V}'_{\text{Coul}}(r) \frac{\mathbf{L}^2}{2r} \left. \right\} + \frac{1}{E_q(E_q + m_q)} \left\{ -(E_q^2 - m_q^2) V_{\text{conf}}^S(r) \right. \\ & \left. + \frac{1}{4} \Delta \left(\hat{V}_{\text{Coul}}(r) - V_{\text{conf}}(r) - 2 \left[\frac{E_q - m_q}{2m_q} - (1 + \kappa) \frac{E_q + m_q}{2m_q} \right] V_{\text{conf}}^V(r) \right) \right\}, \quad (12) \end{aligned}$$

where the diquark and quark energies are defined by their on-mass-shell values [13]

$$E_d = \frac{M^2 - m_q^2 + M_d^2}{2M}, \quad E_q = \frac{M^2 - M_d^2 + m_q^2}{2M}.$$

Here Δ is the Laplace operator, and $\hat{V}_{\text{Coul}}(r)$ is the smeared Coulomb potential which accounts for the diquark internal structure

$$\hat{V}_{\text{Coul}}(r) = -\frac{4}{3} \alpha_s \frac{F(r)}{r}.$$

The spin-dependent potential has the following form [14]

$$V_{\text{SD}}(r) = a_1 \mathbf{L} \mathbf{S}_d + a_2 \mathbf{L} \mathbf{S}_q + b \left[-\mathbf{S}_d \mathbf{S}_q + \frac{3}{r^2} (\mathbf{S}_d \mathbf{r})(\mathbf{S}_q \mathbf{r}) \right] + c \mathbf{S}_d \mathbf{S}_q, \quad (13)$$

where \mathbf{L} is the orbital angular momentum; \mathbf{S}_d and \mathbf{S}_q are the diquark and quark spin operators, respectively. The first two terms are the spin-orbit interactions, the third one is the tensor interaction and the last one is the spin-spin interaction. The coefficients a_1 , a_2 , b and c are expressed through the corresponding derivatives of the smeared Coulomb and confining potentials:

$$\begin{aligned} a_1 = & \frac{1}{M_d(E_d + M_d)} \frac{1}{r} \left[\frac{M_d}{E_d} \hat{V}'_{\text{Coul}}(r) - V'_{\text{conf}}(r) \right] \\ & + \frac{1}{E_d E_q} \frac{1}{r} \left[\hat{V}'_{\text{Coul}}(r) + \frac{E_d}{M_d} \left(\frac{E_d - M_d}{E_q + m_q} + \frac{E_q - m_q}{E_d + M_d} \right) V'_{\text{conf}}(r) \right], \quad (14) \end{aligned}$$

$$\begin{aligned} a_2 = & \frac{1}{E_d E_q} \frac{1}{r} \left\{ \hat{V}'_{\text{Coul}}(r) - \left[\frac{E_q - m_q}{2m_q} - (1 + \kappa) \frac{E_q + m_q}{2m_q} \right] V'_{\text{conf}}(r) \right\} \\ & + \frac{1}{E_q(E_q + m_q)} \frac{1}{r} \left\{ \hat{V}'_{\text{Coul}}(r) - V'_{\text{conf}}(r) - 2 \left[\frac{E_q - m_q}{2m_q} - (1 + \kappa) \frac{E_q + m_q}{2m_q} \right] V'_{\text{conf}}(r) \right\}, \quad (15) \end{aligned}$$

$$b = \frac{1}{3} \frac{1}{E_d E_q} \left\{ \frac{1}{r} \hat{V}'_{\text{Coul}}(r) - \hat{V}''_{\text{Coul}}(r) \right\}, \quad (16)$$

$$c = \frac{2}{3} \frac{1}{E_d E_q} \Delta \hat{V}_{\text{Coul}}(r). \quad (17)$$

Note that both the one-gluon exchange and confining potentials contribute to the quark-diquark spin-orbit interaction. The presence of the spin-orbit $\mathbf{L}\mathbf{S}_q$ and of the tensor terms in the quark-diquark potential (14)–(16) leads to a mixing of states with the same total angular momentum J and parity P but different diquark angular momentum ($\mathbf{L} + \mathbf{S}_d$). We consider such mixing in the same way as in the case of doubly heavy baryons [12].

III. STRANGE BARYON MASSES

We solve numerically the quasipotential equation with the nonperturbative account for the relativistic dynamics both of quarks and diquarks. The calculated values of the ground and excited state baryon masses are presented in Tables II–VIII in comparison with available experimental data [1]. In the first column we show the baryon total spin J and parity P . In the next three columns experimental candidates are listed with their status and measured mass. In the fifth column we give the states of the quark-diquark system in a baryon and the quark-quark state in a diquark for which the following notations are used: $NLnl_j$, where we first show the radial quantum number in the quark-diquark bound system ($N = 1, 2, 3 \dots$) and its orbital momentum by a capital letter ($L = S, P, D \dots$), then the radial quantum number of two quarks in a diquark ($n = 1, 2, 3 \dots$), their orbital momentum by a lowercase letter ($l = s, p, d \dots$) and their total momentum j (the diquark spin) in the subscript. Finally, in the last column our predictions for baryon masses are presented.

From Tables II–VIII we see that most of the observed 3- and 4-star states of strange baryons can be well described as ground and excited states of the quark-diquark bound system in which diquark is in the ground either scalar or axial vector state. However not all of these experimental states can be reproduced. Main deviations from this picture are found in the Λ sector which is better studied experimentally. Indeed the observed $\frac{1}{2}^-$ 4-star states $\Lambda(1405)$ and $\Lambda(1670)$; $\frac{3}{2}^-$ 4-star states $\Lambda(1520)$ and $\Lambda(1690)$; $\frac{1}{2}^+$ 3-star states $\Lambda(1600)$ and $\Lambda(1810)$ as well as $\frac{5}{2}^+$ 4-star $\Lambda(1820)$ and 3-star $\Lambda(2110)$ cannot be simultaneously described in such a simple picture since their mass differences (about 200 MeV) are too small to be attributed to the radial excitations in the quark-diquark bound system amounting to about 500 MeV. Therefore the consideration of excitations inside diquarks is necessary. As we can see from Tables II–VIII the account of diquark excitations allows us to describe all these states and, as a result, to get good agreement of the obtained predictions with data.

In Tables IX–XII we compare the results of our model with previous predictions in various theoretical approaches. The strange baryons were treated in a relativized version of the quark potential model in Ref. [20]. The relativistically covariant quark model based on the Bethe-Salpeter equation with instantaneous two- and three-body forces was employed in Ref. [21]. In Ref. [22] the relativistic quark model with the interquark interaction arising from the meson exchange was used. The authors of Ref. [23] made their calculations of baryon masses below 2 GeV in the relativistic interacting quark-diquark model with the Gürsey and Radicati-inspired exchange interaction. Note that in contrast to our approach, all possible types of ground-state scalar and axial vector diquarks, including qs ($q = u$ or d), were used in Ref. [23], but excitations of diquarks were not considered. Finally, the results of lattice calculations with two light dynamical chirally improved quarks corresponding to pion masses between 255 and 596 MeV [24] are given.

TABLE II: Masses of the positive-parity Λ states (in MeV).

J^P	Experiment [1]			Theory	
	State	Status	Mass	$NLnl_j$	Mass
$\frac{1}{2}^+$	Λ	****	1115.683 ± 0.006	$1S1s_0$	1115
	$\Lambda(1600)$	***	1560 – 1600	$2S1s_0$	1615
	$\Lambda(1710)$	*	1713 ± 13		
	$\Lambda(1810)$	***	1750 – 1810	$1P1p_1$	1901
				$1S2s_0$	1972
				$1P1p_0$	1986
				$1P1p_2$	2042
				$3S1s_0$	2099
				$1P1p_1$	2205
				$2P1p_0$	2431
				$2S2s_0$	2433
				$4S1s_0$	2546
				$2P1p_1$	2559
				$2P1p_2$	2657
			$2P1p_1$	2687	
$\frac{3}{2}^+$	$\Lambda(1890)$	****	1850 – 1890	$1D1s_0$	1854
				$1P1p_2$	1976
				$1P1p_0$	2130
				$1P1p_1$	2184
				$1P1p_2$	2202
				$1P1p_1$	2212
				$2D1s_0$	2289
				$2P1p_0$	2623
				$2P1p_2$	2629
				$2P1p_1$	2690
				$2P1p_1$	2697
				$2P1p_2$	2701
	$\frac{5}{2}^+$	$\Lambda(1820)$	****	1815 – 1820	$1D1s_0$
$\Lambda(2110)$		***	2090 – 2110	$1P1p_2$	2098
				$1P1p_2$	2221
				$1P1p_1$	2255
				$2D1s_0$	2258
				$2P1p_2$	2683
				$2P1p_2$	2724
				$2P1p_1$	2746
$\frac{7}{2}^+$	$\Lambda(2020)$	*	≈ 2020	$1P1p_2$	2251
				$1G1s_0$	2471
				$1F1p_0$	2626
				$2P1p_2$	2744
$\frac{9}{2}^+$	$\Lambda(2350)$	***	2340 – 2350	$1G1s_0$	2360

TABLE III: Masses of the negative-parity Λ states (in MeV).

J^P	Experiment [1]			Theory	
	State	Status	Mass	$NLnl_j$	Mass
$\frac{1}{2}^-$	$\Lambda(1405)$	****	$1405.1^{+1.3}_{-1.0}$	$1P1s_0$	1406
	$\Lambda(1670)$	****	1660 – 1670	$1S1p_1$	1667
	$\Lambda(1800)$	***	1720 – 1800	$1S1p_0$	1733
				$2P1s_0$	1927
				$2S1p_0$	2197
				$1P2s_0$	2218
				$3P1s_0$	2274
				$2S1p_1$	2290
				$1D1p_1$	2427
				$1D1p_2$	2491
$3S1p_0$	2707				
$\frac{3}{2}^-$	$\Lambda(1520)$	****	1519.5 ± 1.0	$1P1s_0$	1549
	$\Lambda(1690)$	****	1685 – 1690	$1S1p_2$	1693
				$1S1p_1$	1812
	$\Lambda(2050)$	*	2056 ± 22	$2P1s_0$	2035
				$1P2s_0$	2319
	$\Lambda(2325)$	*	≈ 2325	$2S1p_2$	2322
				$2S1p_1$	2392
				$3P1s_0$	2454
				$1D1p_0$	2468
				$1D1p_1$	2523
				$1D1p_1$	2546
				$1D1p_2$	2594
$1D1p_2$				2622	
$\frac{5}{2}^-$	$\Lambda(1830)$	****	1810 – 1830	$1S1p_2$	1861
				$1F1s_0$	2136
				$1D1p_0$	2350
				$2S1p_2$	2441
				$1D1p_1$	2549
				$1D1p_1$	2560
				$1D1p_2$	2625
				$1D1p_2$	2639
$\frac{7}{2}^-$	$\Lambda(2100)$	****	2090 – 2100	$1F1s_0$	2097
				$1D1p_1$	2583
				$1D1p_2$	2625
				$1D1p_2$	2639
$\frac{9}{2}^-$				$1D1p_2$	2665
				$1H1s_0$	2738
$\frac{11}{2}^-$				$1H1s_0$	2605

TABLE IV: Masses of the positive-parity Σ states (in MeV).

J^P	Experiment [1]			Theory	
	State	Status	Mass	$NLnl_j$	Mass
$\frac{1}{2}^+$	Σ	****	1189.37 ± 0.07	$1S1s_1$	1187
	$\Sigma(1660)$	***	1630 – 1660	$2S1s_1$	1711
	$\Sigma(1770)$	*	≈ 1770	$1P1p_1$	1922
	$\Sigma(1880)$	*	≈ 1880	$1D1s_1$	1983
				$1S2s_1$	2028
				$1P1p_1$	2180
				$3S1s_1$	2292
				$2D1s_1$	2472
				$2P1p_1$	2515
				$2S2s_1$	2530
				$2P1p_1$	2647
				$1D2s_1$	2672
				$4S1s_1$	2740
	$\frac{3}{2}^+$	$\Sigma(1385)$	****	1382.80 ± 0.35	$1S1s_1$
$\Sigma(1730)$		*	1727 ± 27		
$\Sigma(1840)$		*	≈ 1840	$2S1s_1$	1862
$\Sigma(1940)$		*	1941 ± 18	$1D1s_1$	2025
$\Sigma(2080)$		**	≈ 2080	$1D1s_1$	2076
				$1S2s_1$	2096
				$1P1p_1$	2157
				$1P1p_1$	2186
				$3S1s_1$	2347
				$2D1s_1$	2465
				$2D1s_1$	2483
				$2S2s_1$	2584
				$2P1p_1$	2640
				$2P1p_1$	2654
$\frac{5}{2}^+$	$\Sigma(1915)$	****	1900 – 1915	$1D1s_1$	1991
	$\Sigma(2070)$	*	≈ 2070	$1D1s_1$	2062
				$1P1p_1$	2221
				$2D1s_1$	2459
				$2D1s_1$	2485
				$2P1p_1$	2701
$\frac{7}{2}^+$	$\Sigma(2030)$	****	2025 – 2030	$1D1s_1$	2033
				$2D1s_1$	2470
				$1G1s_1$	2619
$\frac{9}{2}^+$				$1G1s_1$	2548
				$1G1s_1$	2619
$\frac{11}{2}^+$				$1G1s_1$	2529

TABLE V: Masses of the negative-parity Σ states (in MeV).

J^P	Experiment [1]			Theory	
	State	Status	Mass	$NLnl_j$	Mass
$\frac{1}{2}^-$	$\Sigma(1620)$	*	≈ 1620	$1P1s_1$	1620
				$1S1p_1$	1693
	$\Sigma(1750)$	***	1730 – 1750	$1P1s_1$	1747
	$\Sigma(1900)$	*	1900 ± 21	$2P1s_1$	2115
	$\Sigma(2000)$	*	≈ 2000	$2P1s_1$	2198
				$2S1p_1$	2202
				$1P2s_1$	2289
				$1D1p_1$	2381
				$1P2s_1$	2427
				$3P1s_1$	2630
			$3P1s_1$	2634	
			$3S1p_1$	2742	
$\frac{3}{2}^-$	$\Sigma(1580)$	*	≈ 1580		
	$\Sigma(1670)$	***	1665 – 1670	$1P1s_1$	1706
				$1P1s_1$	1731
	$\Sigma(1940)$	***	1900 – 1940	$1S1p_1$	1856
				$2P1s_1$	2175
				$2P1s_1$	2203
				$2S1p_1$	2300
				$1F1s_1$	2409
				$1P2s_1$	2410
				$1P2s_1$	2430
			$1D1p_1$	2494	
			$1D1p_1$	2513	
			$3P1s_1$	2623	
			$3P1s_1$	2637	
$\frac{5}{2}^-$	$\Sigma(1775)$	****	1770 – 1775	$1P1s_1$	1757
				$2P1s_1$	2214
				$1F1s_1$	2347
				$1P2s_1$	2459
				$1F1s_1$	2475
				$1D1p_1$	2516
				$1D1p_1$	2524
				$3P1s_1$	2644
$\frac{7}{2}^-$	$\Sigma(2100)$	*	≈ 2100	$1F1s_1$	2259
				$1F1s_1$	2349
				$1D1p_1$	2545
$\frac{9}{2}^-$			$1F1s_1$	2289	

TABLE VI: Masses of the positive-parity Ξ states (in MeV).

J^P	Experiment [1]			Theory	
	State	Status	Mass	$NLn_l j$	Mass
$\frac{1}{2}^+$	Ξ	****	1321.71 ± 0.07	$1S1s_1$	1330
				$2S1s_1$	1886
				$1D1s_1$	1993
				$1P1p_1$	2012
				$1S2s_1$	2091
				$1P1p_1$	2142
				$3S1s_1$	2367
				$2S2s_1$	2456
				$2D1s_1$	2510
				$1D2s_1$	2565
				$2P1p_1$	2598
				$2P1p_1$	2624
				$\frac{3}{2}^+$	$\Xi(1530)$
$2S1s_1$	1966				
$1D1s_1$	2100				
$1S2s_1$	2121				
$1D1s_1$	2122				
$1P1p_1$	2144				
$1P1p_1$	2149				
$3S1s_1$	2421				
$2S2s_1$	2491				
$2D1s_1$	2597				
$2P1p_1$	2640				
$2D1s_1$	2663				
$2P1p_1$	2664				
$\frac{5}{2}^+$				$1D1s_1$	2108
				$1D1s_1$	2147
				$1P1p_1$	2213
				$2D1s_1$	2605
				$2D1s_1$	2630
$\frac{7}{2}^+$				$1D1s_1$	2189
				$2D1s_1$	2686

From these tables we see that our diquark model predicts appreciably less states than the three-quark approaches. The differences become apparent with the growth of the orbital and radial excitations in the baryon. Our results turn out to be competitive with their predictions for the masses of the well established (4- and 3-star) resonances, which agree well with experimental data. For the less established (1- and 2-star) states situation is more complicated.

TABLE VII: Masses of the negative-parity Ξ states (in MeV).

J^P	Experiment [1]			Theory	
	State	Status	Mass	NLn_l_j	Mass
$\frac{1}{2}^-$				$1P1s_1$	1682
				$1P1s_1$	1758
				$1S1p_1$	1839
				$2P1s_1$	2160
				$2S1p_1$	2210
				$2P1s_1$	2233
				$1P2s_1$	2261
				$1D1p_1$	2346
				$1P2s_1$	2347
$\frac{3}{2}^-$	$\Xi(1820)$	***	1823 ± 5	$1P1s_1$	1764
				$1P1s_1$	1798
				$1S1p_1$	1904
				$2P1s_1$	2245
				$2P1s_1$	2252
				$1P2s_1$	2350
				$1P2s_1$	2352
				$1F1s_1$	2400
				$1D1p_1$	2482
			$1D1p_1$	2506	
$\frac{5}{2}^-$				$1P1s_1$	1853
				$2P1s_1$	2333
				$1P2s_1$	2411
				$1F1s_1$	2455
				$1D1p_1$	2489
				$1D1p_1$	2545
				$1F1s_1$	2569
$\frac{7}{2}^-$				$1F1s_1$	2460
				$1F1s_1$	2474
				$1D1p_1$	2611
$\frac{9}{2}^-$				$1F1s_1$	2502

First we discuss results for the Λ sector. It is necessary to emphasize that the experimental mass of the $\frac{1}{2}^-$ 4-star $\Lambda(1405)$ is naturally reproduced if this state is considered as the first orbital excitation $1P$ in the strange quark-light scalar ($1s_0$) diquark picture of Λ baryons. The rather low mass of this state represents difficulties for most of the three-quark models [20–22], which predict its mass about 100 MeV higher than experimental value. There are no theoretical candidates for the $\frac{1}{2}^+$ 1-star $\Lambda(1710)$ state. The mass of the $\frac{7}{2}^+$ 1-star $\Lambda(2020)$ state is predicted somewhat heavier by all models. Other 1-star Λ states are well described.

In the Σ sector all considered approaches cannot accommodate the $\frac{3}{2}^-$ 1-star $\Sigma(1580)$

TABLE VIII: Masses of the Ω states (in MeV).

J^P	Experiment [1]			Theory		J^P	Theory	
	State	Status	Mass	$NLnl_j$	Mass		$NLnl_j$	Mass
$\frac{1}{2}^+$				$1D1s_1$	2301	$\frac{1}{2}^-$	$1P1s_1$	1941
							$2P1s_1$	2463
							$1P2s_1$	2580
$\frac{3}{2}^+$	Ω	****	1672.45 ± 0.29	$1S1s_1$	1678	$\frac{3}{2}^-$	$1P1s_1$	2038
				$2S1s_1$	2173		$2P1s_1$	2537
				$1S2s_1$	2304		$1P2s_1$	2636
				$1D1s_1$	2332			
				$3S1s_1$	2671			
$\frac{5}{2}^+$				$1D1s_1$	2401	$\frac{5}{2}^-$	$1F1s_1$	2653
$\frac{7}{2}^+$				$1D1s_1$	2369	$\frac{7}{2}^-$	$1F1s_1$	2599
						$\frac{9}{2}^-$	$1F1s_1$	2649

state. The predicted lowest mass $\frac{3}{2}^-$ state corresponds to the 3-star $\Sigma(1670)$ state. We have no candidate for the $\frac{3}{2}^+$ 1-star $\Sigma(1730)$ state in our model. The calculated masses of the 1-star $\frac{1}{2}^+$ $\Sigma(1770)$, $\frac{1}{2}^-$ $\Sigma(1900)$ and $\frac{7}{2}^-$ $\Sigma(2100)$ candidates are by more than 100 MeV heavier than experimentally measured masses. All other known 2- and 1-star Σ states are described with reasonable accuracy.

In the Ξ sector only three (two 4- and one 3-star) states and in the Ω sector only one (4-star) state of the observed baryons have established quantum numbers. They are well described by our model. We have at least one candidate for each of the other eight Ξ (three of them have 3-stars) and three Ω (one of them has 3-stars) states given in PDG Listings [1] with the predicted masses close to the experimental values. However it will be too speculative to assign the quantum numbers to these states only on the basis of their masses. More experimental and theoretical input is needed.

IV. REGGE TRAJECTORIES OF STRANGE BARYONS

In the presented analysis we calculated masses of orbitally excited strange baryons up to rather high orbital excitation numbers: up to $L = 5$ in the quark-diquark bound system, where diquark is in the ground state. This makes it possible to construct the strange baryon Regge trajectories:

$$J = \alpha M^2 + \alpha_0, \quad (18)$$

where α is the slope and α_0 is the intercept.

In Figs. 1-3 we plot the Regge trajectories in the (J, M^2) plane for strange baryons with natural ($P = (-1)^{J-1/2}$) and unnatural ($P = (-1)^{J+1/2}$) parities. The masses calculated in our model are shown by diamonds. Available experimental data are given by dots with error bars and corresponding baryon names. Straight lines were obtained by the χ^2 fit of calculated values. The fitted slopes and intercepts of the Regge trajectories are given in Table XIII. We see that the calculated strange baryon masses lie on the linear trajectories.

TABLE IX: Comparison of theoretical predictions and experimental data for the masses of the Λ states (in MeV).

J^P	Experiment [1]			Theory					
	State	Status	Mass	Our	[20]	[21]	[22]	[23]	[24]
$\frac{1}{2}^+$	Λ	****	1115.683 ± 0.006	1115	1115	1108	1136	1116	1149 ± 18
	$\Lambda(1600)$	***	$1560 - 1600$	1615	1680	1677	1625	1518	1807 ± 94
	$\Lambda(1710)$	*	1713 ± 13						
	$\Lambda(1810)$	***	$1750 - 1810$	1901	1830	1747	1799	1666	2112 ± 54
				1972	1910	1898		1955	2137 ± 69
			1986	2010	2077		1960		
			2042	2105	2099				
			2099	2120	2132				
$\frac{3}{2}^+$	$\Lambda(1890)$	****	$1850 - 1890$	1854	1900	1823		1896	1991 ± 103
				1976	1960	1952			2058 ± 139
				2130	1995	2045			2481 ± 111
				2184	2050	2087			
				2202	2080	2133			
$\frac{5}{2}^+$	$\Lambda(1820)$	****	$1815 - 1820$	1825	1890	1834		1896	
	$\Lambda(2110)$	***	$2090 - 2110$	2098	2035	1999			
				2221	2115	2078			
				2255	2115	2127			
				2258	2180	2150			
$\frac{7}{2}^+$	$\Lambda(2020)$	*	≈ 2020	2251	2120	2130			
				2471		2331			
$\frac{9}{2}^+$	$\Lambda(2350)$	***	$2340 - 2350$	2360		2340			
$\frac{1}{2}^-$	$\Lambda(1405)$	****	$1405.1_{-1.0}^{+1.3}$	1406	1550	1524	1556	1431	1416 ± 81
	$\Lambda(1670)$	****	$1660 - 1670$	1667	1615	1630	1682	1443	1546 ± 110
	$\Lambda(1800)$	***	$1720 - 1800$	1733	1675	1816	1778	1650	1713 ± 116
				1927	2015	2011		1732	2075 ± 249
				2197	2095	2076		1785	
			2218	2160	2117		1854		
$\frac{3}{2}^-$	$\Lambda(1520)$	****	1519.5 ± 1.0	1549	1545	1508	1556	1431	1751 ± 40
	$\Lambda(1690)$	****	$1685 - 1690$	1693	1645	1662	1682	1443	2203 ± 106
				1812	1770	1775		1650	2381 ± 87
	$\Lambda(2050)$	*	2056 ± 22	2035	2030	1987		1732	
				2319	2110	2090		1785	
	$\Lambda(2325)$	*	≈ 2325	2322	2185	2147		1854	
				2392	2230	2259		1928	
				2454	2290	2275		1969	
				2468		2313			
$\frac{5}{2}^-$	$\Lambda(1830)$	****	$1810 - 1830$	1861	1775	1828	1778	1785	
				2136	2180	2080			
				2350	2250	2179			
$\frac{7}{2}^-$	$\Lambda(2100)$	****	$2090 - 2100$	2097	2150	2090			
				2583	2230	2227			
$\frac{9}{2}^-$				2665		2370			

TABLE X: Comparison of theoretical predictions and experimental data for the masses of the Σ states (in MeV).

J^P	Experiment [1]			Theory					
	State	Status	Mass	Our	[20]	[21]	[22]	[23]	[24]
$\frac{1}{2}^+$	Σ	****	1189.37 ± 0.07	1187	1190	1190	1180	1211	1216 ± 15
	$\Sigma(1660)$	***	$1630 - 1660$	1711	1720	1760	1616	1546	2069 ± 74
	$\Sigma(1770)$	*	≈ 1770	1922	1915	1947	1911	1668	2149 ± 66
	$\Sigma(1880)$	*	≈ 1880	1983	1970	2009		1801	2335 ± 63
				2028	2005	2052			
				2180	2030	2098			
				2292	2105	2138			
			2472	2195					
$\frac{3}{2}^+$	$\Sigma(1385)$	****	1382.80 ± 0.35	1381	1370	1411	1389	1334	1471 ± 23
	$\Sigma(1730)$	*	1727 ± 27		1920	1896	1865	1439	
	$\Sigma(1840)$	*	≈ 1840	1862	1970	1961		1924	2194 ± 81
	$\Sigma(1940)$	*	1941 ± 18	2025	2010	2011			2250 ± 79
	$\Sigma(2080)$	**	≈ 2080	2076	2030	2044			2468 ± 67
				2096	2045	2062			
			2157	2085	2103				
			2186	2115	2112				
$\frac{5}{2}^+$	$\Sigma(1915)$	****	$1900 - 1915$	1991	1995	1956		2061	
	$\Sigma(2070)$	*	≈ 2070	2062	2030	2027			
				2221	2095	2071			
$\frac{7}{2}^+$	$\Sigma(2030)$	****	$2025 - 2030$	2033	2060	2070			
				2470	2125	2161			
$\frac{1}{2}^-$	$\Sigma(1620)$	*	≈ 1620	1620	1630	1628	1677	1753	1603 ± 38
				1693	1675	1771	1736	1868	1718 ± 58
	$\Sigma(1750)$	***	$1730 - 1750$	1747	1695	1798	1759	1895	1730 ± 34
	$\Sigma(1900)$	*	1900 ± 21	2115	2110	2111			2478 ± 104
	$\Sigma(2000)$	*	≈ 2000	2198	2155	2136			
				2202	2165	2251			
			2289	2205	2264				
			2381	2260	2288				
$\frac{3}{2}^-$	$\Sigma(1580)$	*	≈ 1580						
	$\Sigma(1670)$	***	$1665 - 1670$	1706	1655	1669	1677	1753	1736 ± 40
				1731	1750	1728	1736	1868	1861 ± 20
	$\Sigma(1940)$	***	$1900 - 1940$	1856	1755	1781	1759	1895	2297 ± 122
				2175	2120	2139			2394 ± 74
			2203	2185	2171				
			2300	2200	2203				
$\frac{5}{2}^-$	$\Sigma(1775)$	****	$1770 - 1775$	1757	1755	1770	1736	1753	
				2214	2205	2174			
				2347	2250	2226			
$\frac{7}{2}^-$	$\Sigma(2100)$	*	≈ 2100	2259	2245	2236			
				2349		2285			
$\frac{9}{2}^-$				2289		2325			

TABLE XI: Comparison of theoretical predictions and experimental data for the masses of the Ξ states (in MeV).

J^P	Experiment [1]			Theory					
	State	Status	Mass	Our	[20]	[21]	[22]	[23]	[24]
$\frac{1}{2}^+$	Ξ	****	1321.71 ± 0.07	1330	1305	1310	1348	1317	1303 ± 13
				1886	1840	1876	1805	1772	2178 ± 48
				1993	2040	2062		1868	2231 ± 44
				2012	2100	2131		1874	2408 ± 45
				2091	2130	2176			
				2142	2150	2215			
				2367	2230	2249			
$\frac{3}{2}^+$	$\Xi(1530)$	****	1531.80 ± 0.32	1518	1505	1539	1528	1552	1553 ± 18
				1966	2045	1988		1653	2228 ± 44
				2100	2065	2076			2398 ± 52
				2121	2115	2128			2574 ± 52
				2122	2165	2170			
				2144	2170	2175			
				2149	2210	2219			
$\frac{5}{2}^+$				2421	2230	2257			
				2108	2045	2013			
				2147	2165	2141			
$\frac{7}{2}^+$				2213	2230	2197			
				2189	2180	2169			
$\frac{1}{2}^-$				1682	1755	1770			1716 ± 43
				1758	1810	1922			1837 ± 28
				1839	1835	1938			1844 ± 43
				2160	2225	2241			2758 ± 78
				2210	2285	2266			
				2233	2300	2387			
				2261	2320	2411			
$\frac{3}{2}^-$	$\Xi(1820)$	***	1823 ± 5	1764	1785	1780	1792	1861	1894 ± 38
				1798	1880	1873		1971	1906 ± 29
				1904	1895	1924			2426 ± 73
				2245	2240	2246			2497 ± 61
				2252	2305	2284			
				2350	2330	2353			
				2352	2340	2384			
$\frac{5}{2}^-$				1853	1900	1955	1881		
				2333	2345	2292			
				2411	2350	2409			
$\frac{7}{2}^-$				2460	2355	2320			
				2474		2425			
$\frac{9}{2}^-$				2502		2505			

TABLE XII: Comparison of theoretical predictions and experimental data for the masses of the Ω states (in MeV).

J^P	Experiment [1]			Theory				
	State	Status	Mass	Our	[20]	[21]	[23]	[24]
$\frac{1}{2}^+$				2301	2220	2232		2350 ± 63
					2255	2256		2481 ± 51
$\frac{3}{2}^+$	Ω	****	1672.45 ± 0.29	1678	1635	1636	1672	1642 ± 17
				2173	2165	2177		2470 ± 49
				2304	2280	2236		
				2332	2345	2287		
$\frac{5}{2}^+$				2401	2280	2253		
					2345	2312		
$\frac{7}{2}^+$				2369	2295	2292		
$\frac{1}{2}^-$				1941	1950	1992		1944 ± 56
				2463	2410	2456		2716 ± 118
				2580	2490	2498		
$\frac{3}{2}^-$				2038	2000	1976		2049 ± 32
				2537	2440	2446		2755 ± 67
				2636	2495	2507		
$\frac{5}{2}^-$				2653	2490	2528		
$\frac{7}{2}^-$				2599		2531		
$\frac{9}{2}^-$				2649		2606		

TABLE XIII: Fitted parameters α , α_0 for the slope and intercept of the (J, M^2) Regge trajectories of strange baryons.

Baryon	α (GeV^{-2})	α_0	Baryon	α (GeV^{-2})	α_0
Λ ($\frac{1}{2}^+$)	0.923 ± 0.016	-0.648 ± 0.057	Λ ($\frac{1}{2}^-$)	0.732 ± 0.018	-0.951 ± 0.074
Σ ($\frac{1}{2}^+$)	0.799 ± 0.029	-0.676 ± 0.100	Σ ($\frac{3}{2}^+$)	0.897 ± 0.010	-0.225 ± 0.037
Ξ ($\frac{1}{2}^+$)	0.694 ± 0.007	-0.721 ± 0.024	Ξ ($\frac{3}{2}^+$)	0.769 ± 0.032	-0.249 ± 0.098
			Ω ($\frac{3}{2}^+$)	0.712 ± 0.002	-0.504 ± 0.007

The natural parity Λ Regge trajectory is the best studied experimentally. There are five well established (four 4-star and one 3-star) states [1] on this trajectory. The masses of these states calculated in our model agree well with data. Using the constructed Regge trajectory we can predict the mass of the $\frac{11}{2}^-$ Λ state to be about 2605 MeV (see Table III). This state could contribute to the $\Lambda(2585)$ bumps observed with the mass ≈ 2585 MeV [1]. Each of the Σ Regge trajectories contains three well established states [1], well fitting to the straight lines. Other trajectories are less motivated experimentally and contain at most two well established states.

Using the values of the slopes and intercepts of the Regge trajectories of the $\frac{3}{2}^+$ strange baryons we can test the validity of the relations between them proposed in the literature

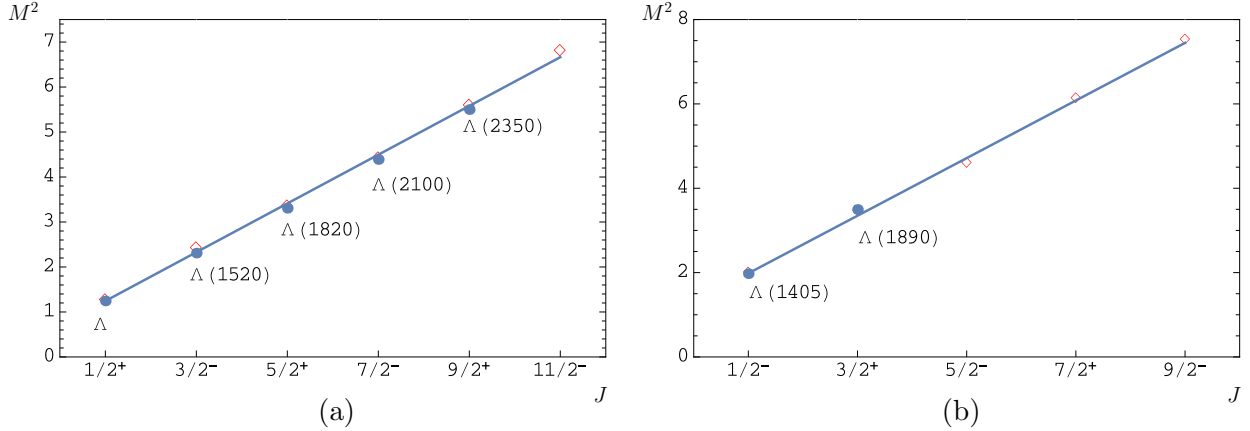


FIG. 1: The (J, M^2) Regge trajectories for the Λ baryons with natural (a) and unnatural (b) parities. Diamonds are predicted masses. Available experimental data are given by dots with particle names; M^2 is in GeV^2 .

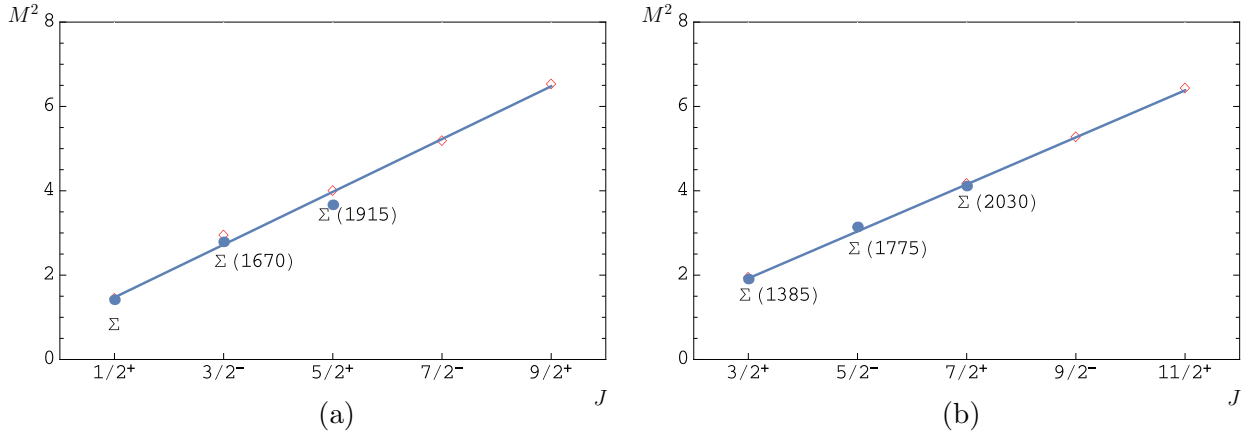


FIG. 2: Same as in Fig. 1 for the Σ baryons.

(see e.g. [25–27] and references therein). It is easy to check that the additivity of inverse slopes

$$\frac{1}{\alpha(\Sigma^*)} + \frac{1}{\alpha(\Omega)} = \frac{2}{\alpha(\Xi^*)}, \quad (19)$$

factorization of slopes

$$\alpha(\Sigma^*)\alpha(\Omega) = \alpha^2(\Xi^*), \quad (20)$$

and additivity of intercepts

$$\alpha_0(\Sigma^*) + \alpha_0(\Omega) = 2\alpha_0(\Xi^*), \quad (21)$$

are well satisfied. Indeed, in the left hand side of Eq. (19) we get 2.52 ± 0.02 and in the right hand side 2.60 ± 0.11 ; for Eq. (20) the corresponding values are 0.639 ± 0.010 and 0.592 ± 0.050 , while for Eq. (21) they are -0.729 ± 0.044 and -0.498 ± 0.196 .

We can also compare the calculated slopes of the strange baryon Regge trajectories with our previous results for the slopes of heavy baryons [14] and light mesons [19]. Such comparison shows that the strange baryon slopes lie just in between the corresponding slopes

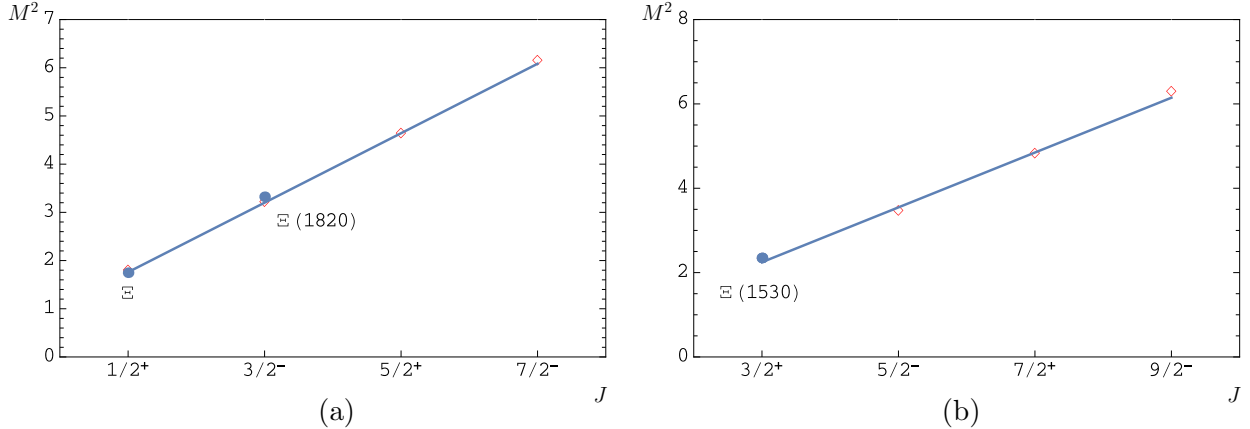


FIG. 3: Same as in Fig. 1 for the Ξ baryons.

of light mesons and charmed baryons. Moreover they follow the same pattern as the slopes of heavy baryons: the slope decreases with the increase of the diquark mass as well as with the increase of the parent baryon mass.

V. CONCLUSIONS

The mass spectra of strange baryons were calculated in the framework of the relativistic quark model based on the quasipotential approach. The quark-diquark picture, which had been previously successfully applied for the investigation of the spectroscopy of heavy baryons [13, 14], was extended to the strange baryons. Such approach allows one to reduce very complicated relativistic three-body problem to the subsequent solutions of two two-body problems. It is assumed that the baryon is the bound quark-diquark system, where two quarks with equal constituent masses form a diquark. The diquarks are not treated to be the point-like objects. Instead their internal structure is taken into account by the introduction of the form factors expressed in terms of the diquark wave functions. The diquark masses and form factors were calculated using the solutions of the relativistic quasipotential equation with the kernel which nonperturbatively accounts for the relativistic effects. It was found that for the correct description of the strange baryon mass spectra it is necessary to consider not only the ground state scalar and axial vector diquarks, as we did in our previous study of heavy baryon spectroscopy [14], but also their first orbital and radial excitations. The ground state and excited baryon masses were obtained by solving the relativistic quark-diquark quasipotential equation. Note that in our analysis we did not make any new assumptions about the quark interaction in baryons or introduce any new parameters. The values of all parameters were taken from previous considerations of meson properties. This significantly increases the reliability and predictive power of our approach. The masses of strange baryons were calculated up to rather high orbital and radial excitations. This allowed us to construct the Regge trajectories which were found to be linear. The validity of the proposed relations between the Regge slopes and intercepts was tested.

The obtained results were compared with available experimental data [1] and previous predictions within different theoretical approaches [20–24]. We found that all 4- and 3-star states of strange baryons with established quantum numbers are well reproduced in our model as well as most of the 2- and 1-star states. Possible candidates for the experimentally

observed states with unknown quantum numbers can be identified. We emphasize that the experimental mass of the $\Lambda(1405)$ is naturally reproduced in our model, while its rather low mass presents some difficulties for most of the three-quark models [20–22]. It is necessary to note that our quark-diquark picture predicts less excited states of strange baryons than the three-body approaches. The distinctions become apparent for higher baryon excitations. However the number of predicted strange baryon states still significantly exceeds the number of observed ones. Thus the experimental determination of the quantum numbers of the already observed Ξ and Ω excited states as well as the further search for the missing excited states of strange baryons represents highly promising and important problem.

Acknowledgments

The authors are grateful to D. Ebert, V. A. Matveev and V. I. Savrin for useful discussions.

-
- [1] K.A. Olive *et al.* (Particle Data Group), *Chin. Phys. C*, **38**, 090001 (2014).
 - [2] N. Brambilla *et al.*, *Eur. Phys. J. C* **71**, 1534 (2011).
 - [3] L. Maiani, F. Piccinini, A. D. Polosa and V. Riquer, *Phys. Rev. D* **71**, 014028 (2005); L. Maiani, F. Piccinini, A. D. Polosa and V. Riquer, *Phys. Rev. D* **89**, no. 11, 114010 (2014).
 - [4] D. Ebert, R. N. Faustov and V. O. Galkin, *Phys. Lett. B* **634**, 214 (2006); *Eur. Phys. J. C* **58**, 399 (2008).
 - [5] R. L. Jaffe, *Phys. Rep.* **409**, 1 (2005).
 - [6] G. 't Hooft, G. Isidori, L. Maiani, A. D. Polosa and V. Riquer, *Phys. Lett. B* **662**, 424 (2008); L. Maiani, F. Piccinini, A. D. Polosa and V. Riquer, *Phys. Rev. Lett.* **93**, 212002 (2004).
 - [7] D. Ebert, R. N. Faustov and V. O. Galkin, *Eur. Phys. J. C* **60**, 273 (2009).
 - [8] E. Klempt and J. M. Richard, *Rev. Mod. Phys.* **82**, 1095 (2010).
 - [9] V. Crede and W. Roberts, *Rept. Prog. Phys.* **76**, 076301 (2013).
 - [10] A. V. Anisovich, V. V. Anisovich, M. A. Matveev, V. A. Nikonov, A. V. Sarantsev and T. O. Vulfs, *Int. J. Mod. Phys. A* **25**, 2965 (2010) [*Int. J. Mod. Phys. A* **25**, 3155 (2010)].
 - [11] H. Forkel and E. Klempt, *Phys. Lett. B* **679**, 77 (2009).
 - [12] D. Ebert, R. N. Faustov, V. O. Galkin and A. P. Martynenko, *Phys. Rev. D* **66**, 014008 (2002).
 - [13] D. Ebert, R. N. Faustov and V. O. Galkin, *Phys. Rev. D* **72**, 034026 (2005); *Phys. Lett. B* **659**, 612 (2008).
 - [14] D. Ebert, R. N. Faustov and V. O. Galkin, *Phys. Rev. D* **84**, 014025 (2011).
 - [15] D. Ebert, R. N. Faustov, V. O. Galkin and A. P. Martynenko, *Phys. Rev. D* **70**, 014018 (2004) [*Phys. Rev. D* **77**, 079903 (2008)].
 - [16] D. Ebert, R. N. Faustov and V. O. Galkin, *Phys. Rev. D* **73**, 094002 (2006).
 - [17] D. Ebert, V. O. Galkin and R. N. Faustov, *Phys. Rev. D* **57**, 5663 (1998) [*Phys. Rev. D* **59**, 019902 (1999)]; *Phys. Rev. D* **67**, 014027 (2003).
 - [18] A.M. Badalian, A.I. Veselov and B.L.G. Bakker, *Phys. Rev. D* **70**, 016007 (2004); Yu.A. Simonov, *Phys. Atom. Nucl.* **58**, 107 (1995).
 - [19] D. Ebert, R. N. Faustov and V. O. Galkin, *Phys. Rev. D* **79**, 114029 (2009).
 - [20] S. Capstick and N. Isgur, *Phys. Rev. D* **34**, 2809 (1986).
 - [21] U. Loring, B. C. Metsch and H. R. Petry, *Eur. Phys. J. A* **10**, 447 (2001).

- [22] T. Melde, W. Plessas and B. Sengl, Phys. Rev. D **77**, 114002 (2008).
- [23] E. Santopinto and J. Ferretti, arXiv:1412.7571 [nucl-th].
- [24] G. P. Engel *et al.* [BGR Collaboration], Phys. Rev. D **87**, no. 7, 074504 (2013).
- [25] A. B. Kaidalov, Z. Phys. C **12**, 63 (1982).
- [26] L. Burakovsky and J. T. Goldman, Phys. Lett. B **434**, 251 (1998).
- [27] X. H. Guo, K. W. Wei and X. H. Wu, Phys. Rev. D **78**, 056005 (2008).